



Published in final edited form as:

Mol Cancer Res. 2010 June ; 8(6): 809–820. doi:10.1158/1541-7786.MCR-09-0460.

Cancer-Associated Fibroblasts derived from EGFR-TKI resistant tumors reverse EGFR pathway inhibition by EGFR-TKIs

Sheldon Mink^{1,2,3}, Surabhi Vashistha^{1,2,3}, Wenxuan Zhang², Amanda Hodge², David B. Agus^{2,4}, and Anjali Jain^{2,3,*}

²Sumner M. Redstone Prostate Cancer Research Program, Cedars-Sinai Medical Center, Los Angeles, California 90048

³Department of Biomedical Sciences, Cedars-Sinai Medical Center, Los Angeles, California 90048

Abstract

Epidermal growth factor receptor (EGFR) plays a critical role in oncogenesis which makes it an attractive target for pharmacological inhibition. Yet, EGFR inhibition with tyrosine kinase inhibitors (TKIs) does not result in a measurable and sustainable clinical benefit in a vast majority of tumors. This emphasizes the need for further investigations into resistance mechanisms against EGFR-TKIs. We previously reported the generation of an *in vivo* adenocarcinoma model of EGFR-TKI acquired resistance that was devoid of the known mechanisms of resistance. Using this same xenograft model, we now demonstrate that the tumor stroma plays an important role in limiting responsiveness to EGFR-TKIs. EGFR-TKI resistant tumors display increased surface expression of CD44^{hi}/CD24^{lo} and markers of epithelial to mesenchymal transition (EMT), *SNAIL* and *N-cadherin*. An *in vivo* GFP-tagging approach reveals that the tumor stroma of the EGFR-TKI resistant tumors is distinct in that 24% of its cancer-associated fibroblast (CAF) population is comprised of EMT-derived tumor cells which represent the *in vivo* escape from EGFR-TKIs. We further demonstrate that EMT subpopulation-harboring CAFs isolated from the EGFR-TKI resistant tumors are tumorigenic and express the biomarker of gefitinib resistance, epithelial membrane protein-1 (EMP-1). Finally, we provide evidence that paracrine factors secreted from the EGFR-TKI resistant CAFs mitigate EGFR-TKI mediated blockade of pEGFR and pMAPK in co-cultured tumor cells, regardless of their EGFR mutational status. This is the first demonstration that the tumor stroma is modified with acquisition of EGFR-TKI resistance and that it further contributes in promoting drug resistance.

Keywords

cancer-associated fibroblasts; EMT; EGFR-TKI; EMP-1

Introduction

Epidermal growth factor receptor (EGFR) kinase signaling pathway plays an integral role in the tumorigenic process of all solid tumors (1,2). This knowledge was the basis for the development of pharmacological kinase inhibitors against EGFR. However, the clinical

*Corresponding Author: Anjali Jain, Ph.D., 8700 Beverly Blvd., Davis 6012, Los Angeles, CA 90048, Tel: 310-423-7376, Fax: 310-423-7699, anjali.jain@cshs.org.

¹These authors contributed equally to this study

⁴Current address: Center for Applied Molecular Medicine, University of Southern California, Los Angeles, CA 90033

Disclosure of potential conflicts of interest: The authors have no potential conflicts of interest to disclose

benefit realized with anti-EGFR treatment is both variable and unpredictable among epithelial cancers. This is attributed to inherent differences in these cancers that hamper a uniform response to such targeted therapeutics. Attempts to identify distinguishing features that select tumors for response have revealed activating somatic mutations (3,4) and gene amplifications (5) within the *EGFR* gene. These features are associated with dramatic clinical responses to EGFR tyrosine kinase inhibitors (TKIs), gefitinib and erlotinib, as they are suggested to enhance the “dependence” of tumor survival on the EGFR pathway. However, such mutations and gene amplifications are primarily limited to a subset of non-small cell lung cancers (NSCLC). Most other solid tumors are modestly dependent upon the EGFR pathway and harbor a non-amplified, wild-type EGFR. Such tumors have demonstrated limited and short-lived responses to EGFR-TKIs in a small number of patients precluding the development of anti-EGFR therapeutics for these cancer types. Well known examples include clinical experiences in renal cell carcinoma (6,7), breast cancer (8), prostate cancer (9), glioblastoma and several others (10). Known features that determine non-response to EGFR-TKIs include pathway gene mutations and alternative signaling pathway activations (3,11–16). However, these mechanisms of EGFR-TKI resistance, which are mostly focused on genetic and post-translational modifications within tumor cells, are not always present in all epithelial cancers that are non-responsive to EGFR-TKIs. This emphasizes that a gap exists in our understanding of factors that limit EGFR-TKI responsiveness and highlights the need to extend investigations into mechanisms of resistance beyond the tumor epithelial cells.

Solid tumor initiation, sustenance and progression is heavily influenced by the supporting stroma or the tumor microenvironment that includes the extracellular matrix (ECM), cancer-associated fibroblasts (CAFs) and the angiogenic component (17–19). Much of the current knowledge, with respect to the role of tumor microenvironment, has been generated from research in epithelial cancers that are dependent on tumor-stromal interactions for survival as demonstrated in breast, prostate and renal cancers (20–22). Coincidentally, these are also the cancer types that have not responded well to EGFR-TKI treatments. Tumor microenvironment is known to limit or modulate therapeutic responses (23) such as to gemcitabine and radiation therapy in pancreatic cancer (24), doxorubicin and cis-platinum in breast and prostate cancer (25), and cisplatin and paclitaxel in ovarian cancer (26). However, it is presently unclear if the tumor microenvironment similarly influences responses to kinase inhibitors such as those targeted to the EGFR.

Cancer-associated fibroblasts are the principal component of the tumor microenvironment that regulate tumor cell function by secreting growth factors, chemokines and ECM (17,21,27). CAFs are typically not considered tumorigenic themselves but rather known to potentiate tumor growth and invasion (28) thereby modulating therapeutic outcome through active signaling cascades with tumor cells (28) and subsequent acquisition of genomic instabilities (29,30). However, the CAF population can also include EMT (epithelial to mesenchymal transition)- or EndMT (endothelial to mesenchymal transition)- derived tumor cells (31–34) which can influence their functional properties. Markers of EMT have been extensively correlated with tumorigenesis (34) but more importantly with therapeutic resistance including that to EGFR-TKIs (12,35,36). Regardless of the tissue of origin, EGFR-TKI resistant tumors expressing EMT markers lack EGFR activating somatic mutations. Ectopic reintroduction of E-cadherin, a marker of the epithelial phenotype, can reverse non-response to EGFR-TKIs (37). These correlative studies suggest that the tumor microenvironment may have a crucial role in governing EGFR-TKI responsiveness in solid tumors; however, a direct demonstration of such a phenomenon has not been reported.

Our group previously reported the derivation of an EGFR-TKI acquired resistance adenocarcinoma model (38) from a xenograft line that was modestly responsive to EGFR

kinase inhibition. The acquired resistance model was devoid of EGFR kinase domain mutations and other known EGFR-TKI resistance mechanisms but overexpressed several markers of the ECM. Using this model, epithelial membrane protein-1 (EMP-1) was identified as a biomarker of gefitinib resistance which was clinically validated in NSCLC samples. In the current study, we present direct evidence that the tumor-associated stroma plays a distinct role in modulating EGFR-TKI responsiveness in this clinically validated model of EGFR-TKI acquired resistance. Specifically, our data show that a sub-population of the CAFs isolated from the EGFR-TKI resistant tumors are a result of EMT and, in collaboration with the host fibroblasts, inhibit EGFR-TKI mediated blockade of the EGFR pathway in co-cultured tumor cells. Overall, our study uncovers a role for tumor-stromal interactions in governing response to EGFR-TKIs.

Materials and Methods

Cell lines and primary tumor ex vivo cultures

Ex vivo tumor cells were cultured in DMEM/F12 medium with 10% FBS. HCC827 NSCLC cells (ATCC) were maintained in RPMI medium containing 10% FBS. CAFs were cultured in stromal cell basal medium (SCBM) with supplements, using the SGBM BulletKit[®] (Lonza).

CAF Isolation

Gefitinib parental (GP) or gefitinib resistant (GR) tumors excised from euthanized mice were rinsed with phenol free RPMI medium (containing 200 U/ml Penicillin and 200 µg/ml of Streptomycin) and enzymatically digested using Collagenase II (100 U/ml) for 5 h at 37° C. The digested tissue was washed and resuspended in SCBM. The epithelial tumor cells were separated from the fibroblasts by a low speed centrifugation method (400 rpm for 5 min) at RT and sorted by FACS using an EpCAM-PE conjugated antibody (BD Biosciences). These cells were the purified epithelial tumor cells. The supernatant from the differential centrifugation of the digested tumor tissue which contained the fibroblasts was gently aspirated, plated in cell culture dishes with fresh SCBM and incubated in a humidified chamber at 37° C with 5% CO₂. Confluent fibroblast cultures were negatively sorted by FACS using the EpCAM-PE conjugated antibody. The data were analyzed using the Cell Quest software version 3.1 (BD Biosciences). These negatively sorted fibroblast cells lacking EpCAM expression were the purified GP or GR CAFs. Immunocytochemistry with fibroblast specific marker, α -Smooth muscle actin (α -SMA), and another epithelial specific marker, E-cadherin, further confirmed the purity of the fibroblasts.

Co-culture and viability assays

For co-culture experiments, HCC827 or the GP tumor cells were plated in the lower chamber of 6 well transwell plates with inserts of pore size 3µm (Costar) and the various CAFs were plated in the accompanying inserts. The tumor cells were treated with the indicated gefitinib concentrations for 24 h. At the assay end point, the tumor cells were harvested and lysed for immunoblotting. Cell viability was analyzed using the CellTiter 96[®] AQueous Non-Radioactive Cell Proliferation Assay colorimetric kit (Promega).

Lentivirus based GFP tagging of tumor cells

pLenti6.3-GFP (Invitrogen) was co-transfected with ViraPower packaging mix (Invitrogen) into 293T cells using Fugene-HD (Roche). 72 h post transfection, the supernatant was collected and filtered through a 0.45 µM cellulose acetate membrane. The GFP-expressing virus was subsequently used to infect 2×10^6 of GP or GR tumor cells at an MOI = 50. 96 h post infection, lentivirus infected cells were dislodged from the culture plates and surface

stained for the epithelial marker, EpCAM. Tumor cells were double sorted for GFP and EpCAM, and $\sim 5 \times 10^4$ of the dual positive tumor cells were mixed 1:1 with matrigel (BD Biosciences), injected subcutaneously into nude mice, and monitored for tumor growth. Upon reaching a tumor volume of $\sim 1000 \text{ mm}^3$, the GFP-expressing tumors were used to isolate the CAFs and tumor cells as described above. CAFs isolated from the GP or GR GFP tumors were subsequently used for immunocytochemical and flow cytometric studies.

Immunoanalysis

Flow cytometric staining of GP and GR tumor cells and CAFs was carried out using the following antibodies: PE-conjugated CD44 (BD Pharmingen), FITC-conjugated CD24 (BD Pharmingen), PE conjugated-EpCAM (BD Biosciences), α -SMA (Sigma), PE-conjugated CDH2 (R & D Systems). Data were analyzed on the MoFlo Cell Sorter (Beckman Coulter Inc.).

For immunoblotting, pEGFR (Cell Signaling), total EGFR (Cell Signaling), pMAPK (Cell Signaling), pAkt (Cell Signaling) antibodies were used with β actin (Sigma) as the normalization control.

For immunofluorescence, GP or GR CAFs were seeded in chamber slides, fixed with 3% PFA in PBS, blocked in 5% goat serum and incubated with antibodies against α -SMA (Sigma) or N-cadherin (BD Biosciences). Post antibody incubation, cells were washed with PBS and incubated with Alexa Fluor 488- or Alexa Fluor 568- conjugated secondary antibodies (Invitrogen) and mounted in Prolong Gold Antifade reagent (Molecular Probes). Cells were stained with the nuclear stain TOPRO-3 or DAPI (Sigma). Confocal microscopy images were acquired at 20 \times or 60 \times magnification and analyzed using Adobe Photoshop.

For immunohistochemistry, GR or GR CAF-derived or GFP-tagged tumors were fixed using 3% PFA and processed for immunohistochemical staining using standard procedures. The samples were probed with antibodies against Ki67 (DakoCytomation), pan-cytokeratin (Biogenex), E-cadherin (BD Biosciences), α -SMA (Sigma) or GFP (AbCam) antibodies. Visualization of immune complexes was performed with a DAB peroxidase substrate kit (Vector Laboratories Inc.) or using Alexa Fluor 488- or Alexa Fluor 568- conjugated secondary antibodies (Invitrogen). The images were acquired using the Leica microscope at 20 \times or 60 \times magnification and analyzed using Adobe Photoshop.

Fluorescence in situ hybridization (FISH)

FISH was performed on methanol fixed GP and GR CAFs. The samples were probed for CEP Y (DYZ1) SpectrumGreen (Abbott Molecular), a probe specific for human Y-chromosome (37). Specificity of the probe was confirmed using mouse sample as the negative control. Co-denaturation and hybridization were performed using the HyBrite machine. Slides were washed and counterstained using the manufacturer's protocol. One hundred interphase nuclei were examined and counted.

Real-time quantitative reverse transcription-PCR

RNA was isolated from tumors using Trizol reagent (Invitrogen) and from cells in culture using the RNeasy Extraction kit (Qiagen). One-Step RT-PCR was performed using AmpliTaq gold pCR Master Mix Reagent (Applied Biosystems) on a 7900HT Sequence Detection System (Applied Biosystems). 100 ng RNA was run in triplicate for each sample in a 384-well plate, normalized to the indicated genes, and analyzed by either the absolute quantification (AQ) or the comparative C_T (RQ) method. The primer and probe sets for *CD44*, *CD24*, *CDH1*, *SNAI2*, *TWIST*, and *ZEB1* were purchased from Applied Biosystems. The sequences for *EMP-1*, *CDH2*, and *SNAI1* used were as follows:

Gene	Forward primer	Reverse primer	Probe
<i>EMP-1</i>	CCAGTGAAGATGCCCTCAA	CCAGGAGGGCAATGACAC	AGTGCAGGCCTTCATGATT
<i>SNAI1</i>	ATCGGAAGCCTAACTACAG	TCCCAGATGAGCATTGG	CTCTAATCCAGAGTTTACCTTCCAGCAGCC
<i>CDH2</i>	TGAAGGTTGCCAGTGTGACT	CAGCACAAGGATAAGCAGGATGAT	CGGGGACTGCACAGATGTGGACAGGATTGT

Xenograft studies

Eight to 10 week-old nude athymic BALB/c female mice were obtained from Charles River Breeding Laboratories and were maintained in pressurized ventilated cages at the Cedars-Sinai Medical Center (CSMC) vivarium. All animal experiments were performed as per the institutional guidelines and approved by the Institutional Animal Care and Use Committee at CSMC. For studying tumor generation from pure CAFs, $\sim 4 \times 10^6$ of the respective fibroblasts purified as per the protocol mentioned above, or $\sim 5 \times 10^4$ cells for the GFP expressing tumor cells, were subcutaneously injected with matrigel (1:1) and tumor growth was monitored. Tumor sizes were measured twice a week with vernier calipers and tumor volumes calculated as: $\pi/6 \times \text{larger diameter} \times (\text{smaller diameter})^2$. Data are represented as a plot of mean tumor volumes versus time in days.

Results

EMP-1, marker of gefitinib resistance, is expressed in the GR CAFs

We previously reported the *in vivo* derivation of a gefitinib resistant (GR) model (38) from an isogenic gefitinib parental (GP) CWR22R xenograft. GP tumors displayed modest but significant tumor growth inhibition ($\sim 63\%$) in presence of gefitinib, as also reported by others (39). Gefitinib responsiveness was rapidly lost when the GP model was passaged in the presence of gefitinib. Unlike the differential responsiveness observed *in vivo*, purified GP and GR epithelial tumor cells had comparable viability in presence of gefitinib (Fig. 1A), indicating a role for the tumor microenvironment in modulating EGFR-TKI response. As expected, inhibition of pEGFR and pMAPK was minimal with gefitinib in line with the limited dependency of this model on the EGFR pathway (Fig 1B). This prompted us to isolate and characterize the CAFs from GP and GR tumors. Isolated CAFs were confirmed for their purity by the absence of epithelial-specific markers, EpCAM (Supplementary Fig. S1) and E-cadherin, and presence of the fibroblast-specific marker, α -SMA (Supplementary Fig. S2). The definition and composition of CAFs remains relatively poorly defined with some groups favoring a functional definition i.e., activated fibroblasts that promote tumorigenicity (27,40). However, in this study, we define CAFs based on their fibroblastic morphology and expression of mesenchymal markers such as α -SMA with a simultaneous absence of epithelial cell markers. This definition of CAFs based on morphology and fibroblast marker expression has been previously described and typically includes cells derived as a result of EMT or EndMT (31–33).

As another indicator of fibroblast purity, a quantitative RT-PCR for *EMP-1* was performed on the purified GP and GR CAFs using both human- and murine-specific gene primers. We were surprised to note that while murine *EMP-1* (*mEMP-1*) mRNA levels were comparable between GP and GR CAFs (data not shown); human *EMP-1* (*hEMP-1*) was overexpressed in the GR CAFs by ~ 45 -fold (Fig. 1C) as compared to the GP CAFs. Expression of *hEMP-1* in the GR CAFs implied the presence of human fibroblasts amongst the murine fibroblast population. This observation was further confirmed by comparative FISH analysis using CEP Y (DYZ1), a human Y-chromosome specific probe (41), which demonstrated that the

GP CAFs were exclusively murine whereas ~15% of the GR CAFs were of human origin (Fig. 1D, compare the nuclei indicated in white (human) or red (murine) arrows). These data provide clear evidence that human fibroblast population characterized by *hEMP-1* expression exists within the murine stroma of the EGFR-TKI resistant GR tumors, supporting the notion of an epithelial origin for this fibroblast sub-population.

EGFR-TKI resistant GR tumors express mesenchymal markers and CD44^{hi}/CD24^{lo} cell surface expression

The tumor cell morphology was comparable between the purified GP and GR epithelial tumor cells (Fig. 2A). Since the GR CAFs include a human-specific sub-population, a plausible explanation was that these cells might have originated from the GR tumor cells via an EMT event. To explore this possibility, we compared the expression of classical EMT markers in the *ex vivo* derived GP and GR epithelial tumor cells. Quantitative mRNA analyses revealed that the mesenchymal marker, human *CDH2* (*N-cadherin*), was expressed ~8–10 fold higher in the GR tumor cells (Fig. 2B, top panel), as compared to the GP counterparts. However, mRNA expression of the epithelial marker, human *CDH1* (*E-cadherin*), was comparable between the GP and GR epithelial tumor cells (Fig. 2B, middle panel). We also analyzed the cell surface CDH1 and CDH2 protein expression in GP and GR epithelial tumor cells. While cell surface CDH1 protein expression was comparable between GP and GR epithelial tumor cells (data not shown), a higher percentage (25.6%) of GR epithelial tumor cells expressed CDH2 (Fig. 2C) than the GP epithelial tumor cells (0.8%). Furthermore, comparative mRNA analyses of the key transcription factors that regulate EMT i.e., *SNAI1*, *SNAI2*, *ZEB1* and *TWIST*, revealed ~5–10 fold overexpression of *SNAI1* in three different isolates of GR epithelial tumor cells (Fig. 2B, bottom panel). The other transcription factors, *SNAI2*, *ZEB1* and *TWIST*, did not display a consistent expression pattern in three different isolates of GP and GR epithelial tumor cells (Supplementary Fig. S3).

EMT induction is linked with acquisition of CD44^{hi}/CD24^{lo} cell surface expression (42). We observed a higher (84.64%) CD44^{hi}/CD24^{lo} population in the GR epithelial tumor cells whereas only 1.56% was detected in the GP epithelial tumor cells (Fig. 2D). Further, we compared *CD44* and *CD24* mRNA expression in three separate isolates of GP and GR epithelial tumor cells. Alongside, we also examined tumor cells derived from an isogenic paclitaxel-resistant model which was also derived from the parental CWR22R xenograft (Jain et al., unpublished data). As shown in Supplementary Fig. S4, *CD44* mRNA was expressed at two orders of magnitude higher in GR epithelial tumor cells as compared to the GP counterparts while *CD24* expression remained unchanged. The paclitaxel-resistant cells did not overexpress *CD44*. These cells also failed to overexpress the EMT markers observed in the GR model (data not shown).

Taken together, these analyses indicate the possible occurrence of EMT in the GR model. Furthermore, presence of an explicit CD44^{hi}/CD24^{lo} cell surface signature, specifically in the GR tumor cells that are presumably undergoing EMT, is suggestive of a link between the two phenomena in this EGFR-TKI non-responsive model.

EGFR-TKI resistant GR tumors undergo EMT

Our observations thus far indicate the occurrence of EMT in the GR tumors; however, a direct demonstration is lacking. Therefore we tagged both *ex-vivo* GP and GR epithelial tumor cells with GFP, co-sorted them with EpCAM positive cells to ascertain epithelial cell purity and injected them subcutaneously into nude mice with the idea that if EMT is occurring then the CAFs in the resulting tumors would be GFP-positive (procedure outlined in Supplementary Fig. S5). Consistent with our hypothesis, GFP expression was observed in

a subset of purified GR CAFs after the GR tumors grew out (Fig. 3A). Co-expression of two different mesenchymal markers, α -SMA and N-cadherin, with GFP confirmed the mesenchymal lineage of the GFP positive GR CAFs which thus demonstrated that these cells were indeed the result of an *in vivo* EMT event (Fig. 3B). Immunohistochemical staining of paraffin-embedded sections of the tumor also revealed a co-localization of GFP and the mesenchymal marker, α -SMA, specifically in the GR tumors (Fig. 3D, compare c and f). A closer inspection of the GFP-expressing mesenchymal cells derived from GR tumors revealed that their morphology was very different from the host fibroblasts in that their phenotype appeared at an intermediate stage between an epithelial and a mesenchymal cell morphology (Fig. 3B). Their nuclei had a diffused DAPI staining pattern (characteristic of human nuclei) as opposed to the punctate staining of the host murine nuclei (Fig. 3B, d and h) (43). Although this analysis revealed the presence of EMT-derived CAFs within the GR tumors, an overall comparative morphologic and immunohistochemical evaluation suggested similar epithelial to stromal ratios in the GP and GR tumors (Fig. 3C).

Next, we determined the percentage of the EMT undergoing GFP cells within the GR CAFs. Flow cytometric analysis of the GP and GR CAFs with co-expression of α -SMA and GFP indicated that unlike the GP CAFs, 23.9% of the GR CAFs were dual positive for GFP and high α -SMA expression (Fig. 3E). This cell percentage is a little bit higher than what was estimated by FISH analysis (Fig. 1D), which could be due to the difference in sensitivity of the two techniques. Overall, these studies demonstrate that the GR tumors, but not the GP tumors, undergo EMT and that a sub-population of the GR CAFs comprises the EMT-undergoing GR tumor cells.

GR CAFs are tumorigenic

We next asked if the EMT-derived GR CAFs maintain their tumorigenicity while they are resident within the host fibroblast population. To test this, equivalent numbers of purified GP and GR CAFs were subcutaneously injected into immunodeficient mice and monitored for tumor growth. Two independent isolates of the CAFs were used. Equivalent numbers of GR epithelial tumor cells or fibroblasts derived from a naïve nude mouse were also transplanted in parallel. Of the three types of fibroblast transplants (GP, GR or naïve), only the GR CAFs gave rise to palpable tumors after ~21 to 25 days (Fig. 4A). Tumors derived from the GR CAFs had approximately a 3-fold longer latency period as compared to the GR tumors. Immunohistochemical analysis of the GR CAF-derived tumors revealed that the tumors were epithelial (E-cadherin positive) and genotypically human (positive for human-specific pan-cytokeratin), thus demonstrating that the GR CAFs are tumorigenic (Fig. 4B, g and h respectively). GR CAF-derived tumors were histologically similar to the GR tumors (Fig. 4B, compare a and e) and were actively proliferating as demonstrated by positive Ki-67 expression (Fig. 4B, f).

Based on the *hEMP-1* expression in the GR CAFs (Fig. 1C), we expected the GR CAF-derived tumors to also express *hEMP-1*. Indeed the GR CAF-derived tumors expressed *hEMP-1* mRNA at levels comparable to the GR CAFs (Fig. 4C). Our data therefore strongly suggest that EMP-1, besides being a biomarker of gefitinib resistance, also identifies the EMT undergoing tumorigenic cell population within the GR tumors.

pEGFR and pMAPK are inefficiently blocked with EGFR-TKIs in presence of GR CAFs

Since GR CAFs were derived from tumors that had acquired resistance to EGFR-TKIs, we wanted to examine if the GR CAFs had any influence on EGFR-TKI activity. We addressed this by directly evaluating the effect of gefitinib on the molecular correlates of the EGFR activity (i.e. pEGFR) and its downstream effectors (i.e. pMAPK and pAkt) in gefitinib sensitive cells when they were co-cultured in presence of GR CAFs.

GP epithelial tumor cells (Fig. 5A) were co-cultured with GP or GR CAFs in presence of gefitinib for 24 hours before EGFR pathway analysis. In presence of the GP CAFs, gefitinib treatment resulted in a similar inhibition of the pEGFR signal as in the presence of media alone (compare lanes 1 and 2 to 3 and 4). In contrast, presence of the GR CAFs caused a resistance to gefitinib-mediated pEGFR inhibition (40% inhibition in presence of GR CAFs as compared to 73% inhibition in presence of GP CAFs, compare lanes 3 and 4 to lanes 5 and 6). Since the GP tumor cells are modestly dependent on the EGFR pathway (Fig. 1A and 1B) and harbor a wild-type EGFR which is not gene amplified, EGFR kinase inhibition at the pMAPK and pAkt levels was minor, if any. This was also the reason why we needed to utilize high gefitinib concentrations in this assay. We next wanted to examine if the differences in the effects of GP and GR CAFs would also be demonstrated in other gefitinib sensitive systems that are highly dependent upon the EGFR pathway. Therefore we investigated the influence of GR CAF co-culture on a NSCLC cell line, HCC827. HCC827 cells carry a deletion mutation within the *EGFR* gene, E746-A750, which makes them ultra-sensitive to EGFR-TKIs. The differences between the GP and GR CAFs were even more pronounced in the HCC827 cells as their effects were observed on the downstream effectors of the EGFR pathway. As shown in Fig. 5B, 100nM of gefitinib caused >50% inhibition of the pMAPK signal in presence of the GP CAFs while the presence of the GR CAFs resulted in less than a 15% inhibition. Differences at the level of pEGFR were minor due to the presence of EGFR mutations that increase the affinity of EGFR-TKIs (4). No changes were observed in Akt phosphorylation.

Our data clearly demonstrate that the presence of the CAFs, derived from the EGFR-TKI resistant tumors, significantly compromises EGFR-TKI activity. These data highlight the fact that, in addition to the tumor cells, the stroma in the EGFR-TKI resistant tumors is differentially programmed such that it can limit EGFR-TKI activity in the neighboring tumor cells.

Discussion

We have utilized a unique isogenic pair of a prostate adenocarcinoma model with a limited dependency on the EGFR signaling pathway and its EGFR-TKI resistant counterpart to uncover novel features of EGFR-TKI acquired resistance. Utilizing this model pair, we had previously reported the identification of EMP-1 as a biomarker of EGFR-TKI resistance that was validated in EGFR-TKI resistant lung cancer clinical samples (38). Data presented in this study demonstrates that, in addition to the tumor cells, the tumor microenvironment is also modulated as the tumors acquire resistance to EGFR-TKIs. The modified tumor microenvironment then plays a role in limiting tumor responsiveness to EGFR-TKIs.

We provide evidence that acquired resistance to EGFR-TKI treatment leads to enrichment of EMT undergoing tumor cells with a CD44^{hi}/CD24^{lo} cell surface expression. The tumor cells, that undergo EMT with acquisition of EGFR-TKI resistance, reside within the surrounding CAF population of the EGFR-TKI resistant tumors. The CAF population derived from the GR tumors can mitigate EGFR-TKI mediated EGFR pathway kinase inhibition in tumor cells. The EMT-enriched tumor population in the GR tumors, which represent the *in vivo* escape from EGFR-TK inhibition, is marked by EMP-1. Notably, the findings described in our study are specific to EGFR-TKI resistance and were not observed in an isogenic tumor model which is resistant to the taxane-based chemotherapeutic agent, paclitaxel.

Several reports have previously correlated the EMT markers with non-responsiveness to EGFR-TKIs (12,35). We demonstrate that EGFR kinase inhibition accelerates the selection of EMT undergoing cells in tumors with a limited dependency on the EGFR pathway that

ultimately leads to acquired resistance to EGFR TKIs. Tumor cells undergoing EMT potentially camouflage themselves within the tumor microenvironment i.e., the GR CAFs to escape EGFR-TKI exposure. Interestingly, according to our data the EMT-derived tumor cells within the GR CAFs maintain their tumorigenicity and are able to grow out as epithelial tumors most likely by utilizing the reverse EMT phenomenon of mesenchymal to epithelial transition (MET). We did observe a significant delay in subcutaneous tumor growth from the GR CAFs as compared to the GR tumor cells. This time lag may have been due to the reverse transition of the mesenchymal cells to an epithelial phenotype, as the resulting tumors were epithelial in nature. Existence of an EMT-MET program specifically in the GR tumors implies that the enrichment of EMT-undergoing cells likely plays an active role in the maintenance and progression of EGFR-TKI resistance instead of being a bystander effect of therapeutic non-response. There is precedence for the role of EMT in maintaining tumorigenicity (44,45). In addition to the EMT markers, we also observe EMP-1 expression on the EMT-undergoing GR mesenchymal cells. Upregulation of EMP-1 family members have been demonstrated in erlotinib-insensitive lung cancer cell lines expressing EMT markers by our group and others (12). Whether EMP-1 has a direct involvement in the EMT process as a result of EGFR-TKI resistance is still unknown. However, it is known that *EMP-1* is a c-myc target gene (46) and c-myc-driven mouse mammary tumors can elicit EMT (47).

Induction of EMT in the GR model is likely due to the upregulation of the *SNAIL* transcription factor. An important question is the identity of specific upstream signals that upregulate *SNAIL* to initiate EMT within the GR tumors. EMT can be induced by a multitude of signals (48). Our attempts at inducing TGF β -mediated EMT in *ex vivo* GP tumor cells have been unsuccessful. It is plausible that chronic gefitinib treatment initiated the EMT phenomenon in the GR tumors by activating compensatory growth signaling pathways. Activation of such pathways (14,15) is emerging as a generalized escape mechanism that the tumors employ to evade treatment with kinase-specific small molecule inhibitors.

GR tumor cells undergoing EMT display a CD44^{hi}/CD24^{lo} cell surface expression. CD44^{hi}/CD24^{lo} sub-populations are suggested to mark putative cancer stem cell populations in both breast (49) and prostate cancers (50) that are implicated with treatment resistance (51). Therefore, it is possible to speculate that GP tumors harbor a pre-existing CD44^{hi}/CD24^{lo} cancer stem cell population which escapes EGFR-TKI response and is enriched for in the GR tumors. However, tumor cells from an isogenic paclitaxel-resistant model did not select for CD44^{hi}/CD24^{lo} expression or EMT markers thus arguing against the idea of a simple enrichment process of cancer stem cells in the GR model. Recent reports (42,52) demonstrate that EMT stimulates cancer cells to adopt stem cell-like characteristics with a CD44^{hi}/CD24^{lo} surface phenotype. We believe that a similar scenario may exist in the GR model with the acquisition of gefitinib resistance and EMT. Although our evidence for a stem cell-like phenotype in the GR model is preliminary, it is provocative to suggest that the acquisition of stem cell-like phenotype might cooperate with the EMT program in the maintenance of EGFR-TKI resistance while amplifying the resistant tumor population.

Besides the occurrence of EMT and an enriched CD44^{hi}/CD24^{lo} phenotype, the CAF population in the GR tumors is also unique. Paracrine factors secreted from the GR CAFs diminish EGFR-TKI dependent inhibition of the EGFR pathway in the neighboring tumor cells independent of the presence of EGFR activating mutations. The GR CAFs include an EMT-derived sub-population and the GFP tagging strategy clearly indicates that this sub-population maintains a distinct morphology within the mass of host fibroblasts. It remains to be investigated if it is only the EMT-derived GR CAFs or the entire GR CAF population that plays a role in influencing EGFR-TKI non-responsiveness in the neighboring tumor

cells. Genomic instabilities within CAFs are documented to modulate their function (29,30). Future studies delineating the identity of the genetic modifications and the paracrine factors secreted by the GR CAFs will help decipher their role in EGFR-TKI non-responsiveness.

In summary, our study is the first comprehensive examination of the tumor-associated stroma in tumors that have acquired resistance to EGFR-TKIs. It suggests that acquired resistance mechanisms to EGFR-TKIs extend beyond the cancer cell and involve reprogramming of the tumor microenvironment, in addition to the tumor cells. Furthermore, our findings highlight the need for investigations for potential targets within cancer-associated fibroblasts (53) to counter EGFR-TKI resistance.

Supplementary Material

Refer to Web version on PubMed Central for supplementary material.

Acknowledgments

We thank Drs. Leland Chung (Cedars-Sinai Medical Center), Donna Peehl (Stanford University) and Georg F. Weber (University of Cincinnati) for critical review and helpful suggestions. Technical assistance from Dr. Rhona Schreck and Kevin Baden (cytogenetics work), Dan Luthringer and Ganghua Huang (IHC stainings), Patricia Lin (flow cytometry), Kolja Wawrowsky (confocal microscopy) and John Curran (qRT-PCR analysis) is gratefully acknowledged.

Grant support: Jerry and Joyce Monkarsh Young Investigator Award (Prostate Cancer Foundation; A. J.), the National Institutes of Health 1-R21 NS059381-01 (A. J.) and Sumner Redstone Prostate Cancer Research Program (D. B. A. and A. J.).

References

1. Gschwind A, Fischer OM, Ullrich A. The discovery of receptor tyrosine kinases: targets for cancer therapy. *Nat Rev Cancer*. 2004; 4:361–370. [PubMed: 15122207]
2. Hynes NE, Lane HA. ERBB receptors and cancer: the complexity of targeted inhibitors. *Nat Rev Cancer*. 2005; 5:341–354. [PubMed: 15864276]
3. Ciardiello F, Tortora G. EGFR antagonists in cancer treatment. *The New England journal of medicine*. 2008; 358:1160–1174. [PubMed: 18337605]
4. Sharma SV, Bell DW, Settleman J, Haber DA. Epidermal growth factor receptor mutations in lung cancer. *Nat Rev Cancer*. 2007; 7:169–181. [PubMed: 17318210]
5. Tsao MS, Sakurada A, Cutz JC, et al. Erlotinib in lung cancer - molecular and clinical predictors of outcome. *The New England journal of medicine*. 2005; 353:133–144. [PubMed: 16014883]
6. Dawson NAGC, Zak R, Dorsey B, Smoot J, Wong J, Hussain A. A phase II trial of gefitinib (Iressa, ZD1839) in stage IV and recurrent renal cell carcinoma. *Clin Cancer Res*. 2004; 10:7812–7819. [PubMed: 15585612]
7. Jermann MSR, Salzberg M, Cerny T, Joerger M, Gillessen S, Morant R, Egli F, Rhyner K, Bauer JA, Pless M. A phase II, open-label study of gefitinib (IRESSA) in patients with locally advanced, metastatic, or relapsed renal-cell carcinoma. *Cancer Chemother Pharmacol*. 2006; 57:533–539. [PubMed: 16052341]
8. Baselga JAJ, Ruiz A, Lluch A, Gascón P, Guillém V, González S, Sauleda S, Marimón I, Tabernero JM, Koehler MT, Rojo F. Phase II and tumor pharmacodynamic study of gefitinib in patients with advanced breast cancer. *J Clin Oncol*. 2005; 23:5323–5333. [PubMed: 15939921]
9. Canil CMMM, Winkvist E, Baetz T, Pollak M, Chi KN, Berry S, Ernst DS, Douglas L, Brundage M, Fisher B, McKenna A, Seymour L. Randomized phase II study of two doses of gefitinib in hormone-refractory prostate cancer: a trial of the National Cancer Institute of Canada-Clinical Trials Group. *J Clin Oncol*. 2005; 23:455–460. [PubMed: 15659491]
10. Cappuzzo F, Finocchiaro G, Metro G, et al. Clinical experience with gefitinib: an update. *Critical reviews in oncology/hematology*. 2006; 58:31–45. [PubMed: 16531062]

11. Ji HZX, Yuza Y, Shimamura T, Li D, Protopopov A, Jung BL, McNamara K, Xia H, Glatt KA, Thomas RK, Sasaki H, Horner JW, Eck M, Mitchell A, Sun Y, Al-Hashem R, Bronson RT, Rabindran SK, Discafani CM, Maher E, Shapiro GI, Meyerson M, Wong KK. Epidermal growth factor receptor variant III mutations in lung tumorigenesis and sensitivity to tyrosine kinase inhibitors. *Proc Natl Acad Sci U S A*. 2006; 103:7817–7822. [PubMed: 16672372]
12. Yauch RLJT, Eberhard DA, Cavet G, Zhu W, Fu L, Pham TQ, Soriano R, Stinson J, Seshagiri S, Modrusan Z, Lin CY, O'Neill V, Amler LC. Epithelial versus mesenchymal phenotype determines in vitro sensitivity and predicts clinical activity of erlotinib in lung cancer patients. *Clin Cancer Res*. 2005; 11:8686–8698. [PubMed: 16361555]
13. Sergina NVRM, Wang D, Blair J, Hann B, Shokat KM, Moasser MM. Escape from HER-family tyrosine kinase inhibitor therapy by the kinase-inactive HER3. *Nature Reviews Cancer*. 2007; 445:437–441.
14. Morgillo FWJ, Kim ES, Hong WK, Lee HY. Heterodimerization of insulin-like growth factor receptor/epidermal growth factor receptor and induction of survivin expression counteract the antitumor action of erlotinib. *Cancer Res*. 2006; 66:10100–10111. [PubMed: 17047074]
15. Christensen JGSR, Chan E, Wang X, Yang C, Liu L, Cui J, Sun L, Wei J, Cherrington JM, Mendel DB. High levels of HER-2 expression alter the ability of epidermal growth factor receptor (EGFR) family tyrosine kinase inhibitors to inhibit EGFR phosphorylation in vivo. *Clin Cancer Res*. 2001; 7:4230–4238. [PubMed: 11751524]
16. Engelman JAJ. Mechanisms of acquired resistance to epidermal growth factor receptor tyrosine kinase inhibitors in non-small cell lung cancer. *Clin Cancer Res*. 2008; 14:2895–2899. [PubMed: 18483355]
17. Olumi AFGG, Hayward SW, Carroll PR, Tlsty TD, Cunha GR. Carcinoma-associated fibroblasts direct tumor progression of initiated human prostatic epithelium. *Cancer Res*. 1999; 59:5002–5011. [PubMed: 10519415]
18. Marastoni SLG, Lorenzon E, Colombatti A, Mongiat M. Extracellular matrix: a matter of life and death. *Connect Tissue Res*. 2008; 49:203–206. [PubMed: 18661343]
19. Chung LWBA, Assikis V, Zhau HE. Molecular insights into prostate cancer progression: the missing link of tumor microenvironment. *J Urol*. 2005; 173:10–20. [PubMed: 15592017]
20. Taylor RARG. Prostatic tumor stroma: a key player in cancer progression. *Curr Cancer Drug Targets*. 2008; 8:490–497. [PubMed: 18781895]
21. Orimo AGP, Sgroi DC, Arenzana-Seisdedos F, Delaunay T, Naeem R, Carey VJ, Richardson AL, Weinberg RA. Stromal fibroblasts present in invasive human breast carcinomas promote tumor growth and angiogenesis through elevated SDF-1/CXCL12 secretion. *Cell*. 2005; 121:335–348. [PubMed: 15882617]
22. Wysocki PJ, Zolnieriek J, Szczylik C, Mackiewicz A. Targeted therapy of renal cell cancer. *Curr Opin Investig Drugs*. 2008; 9:570–575.
23. Tredan O, Galmarini CM, Patel K, Tannock IF. Drug resistance and the solid tumor microenvironment. *Journal of the National Cancer Institute*. 2007; 99:1441–1454. [PubMed: 17895480]
24. Hwang RFMT, Arumugam T, Ramachandran V, Amos KD, Rivera A, Ji B, Evans DB, Logsdon CD. Cancer-associated stromal fibroblasts promote pancreatic tumor progression. *Cancer Res*. 2008; 68:918–926. [PubMed: 18245495]
25. Lafkas DTG, Papavassiliou AG, Kiaris H. P53 mutations in stromal fibroblasts sensitize tumors against chemotherapy. *Int J Cancer*. 2008; 123:967–971.
26. Rafii AMP, Poupot M, Faussat AM, Simon A, Ducros E, Mery E, Couderc B, Lis R, Capdet J, Bergalet J, Querleu D, Dagonnet F, Fournié JJ, Marie JP, Pujade-Lauraine E, Favre G, Soria J, Mirshahi M. Oncologic trogocytosis of an original stromal cells induces chemoresistance of ovarian tumours. *PLoS ONE*. 2008; 3:e3894. [PubMed: 19079610]
27. Bhowmick NA, Neilson EG, Moses HL. Stromal fibroblasts in cancer initiation and progression. *Nature*. 2004; 432:332–337. [PubMed: 15549095]
28. Boire ACL, Agarwal A, Jacques S, Sherifi S, Kuliopulos A. PAR1 is a matrix metalloprotease-1 receptor that promotes invasion and tumorigenesis of breast cancer cells. *Cell*. 2005; 120:303–313. [PubMed: 15707890]

29. Fukino KSL, Patocs A, Mutter GL, Eng C. Genomic instability within tumor stroma and clinicopathological characteristics of sporadic primary invasive breast carcinoma. *JAMA*. 2007; 297:2103–2111. [PubMed: 17507346]
30. Pelham RJRL, Hall I, Lucito R, Nguyen KC, Navin N, Hicks J, Mu D, Powers S, Wigler M, Botstein D. Identification of alterations in DNA copy number in host stromal cells during tumor progression. *Proc Natl Acad Sci U S A*. 2006; 103:19848–19853. [PubMed: 17167050]
31. Kalluri R, Weinberg RA. The basics of epithelial-mesenchymal transition. *The Journal of clinical investigation*. 2009; 119:1420–1428. [PubMed: 19487818]
32. Ostman A, Augsten M. Cancer-associated fibroblasts and tumor growth--bystanders turning into key players. *Current opinion in genetics & development*. 2009; 19:67–73. [PubMed: 19211240]
33. Kalluri RZM. Fibroblasts in cancer. *Nat Rev Cancer*. 2006; 6:392–401. [PubMed: 16572188]
34. Potenta SZE, Kalluri R. The role of endothelial-to-mesenchymal transition in cancer progression. *Br J Cancer*. 2008; 99:1375–1379. [PubMed: 18797460]
35. Thomson SBE, Petti F, Griffin G, Brown E, Ramnarine N, Iwata KK, Gibson N, Haley JD. Epithelial to mesenchymal transition is a determinant of sensitivity of non-small-cell lung carcinoma cell lines and xenografts to epidermal growth factor receptor inhibition. *Cancer Res*. 2005; 65:9455–9462. [PubMed: 16230409]
36. Frederick BAHB, Coldren CD, Zheng D, Chan D, Bunn PA Jr, Raben D. Epithelial to mesenchymal transition predicts gefitinib resistance in cell lines of head and neck squamous cell carcinoma and non-small cell lung carcinoma. *Mol Cancer Ther*. 2007; 6:1683–1691. [PubMed: 17541031]
37. Witta SEGR, Hirsch FR, Coldren CD, Hedman K, Ravdel L, Helfrich B, Dziadziuszko R, Chan DC, Sugita M, Chan Z, Baron A, Franklin W, Drabkin HA, Girard L, Gazdar AF, Minna JD, Bunn PA Jr. Restoring E-cadherin expression increases sensitivity to epidermal growth factor receptor inhibitors in lung cancer cell lines. *Cancer Res*. 2006; 66:944–950. [PubMed: 16424029]
38. Jain ATC, Laux I, Hunter JB, Curran J, Galkin A, Afar DE, Aronson N, Shak S, Natale RB, Agus DB. Epithelial membrane protein-1 is a biomarker of gefitinib resistance. *Proc Natl Acad Sci U S A*. 2005; 102:11858–11863. [PubMed: 16087880]
39. Sirotnak FMSY, Lee F, Chen J, Scher HI. Studies with CWR22 xenografts in nude mice suggest that ZD1839 may have a role in the treatment of both androgen-dependent and androgen-independent human prostate cancer. *Clin Cancer Res*. 2002; 8:3870–3876. [PubMed: 12473602]
40. Tuxhorn JA, Ayala GE, Rowley DR. Reactive stroma in prostate cancer progression. *The Journal of urology*. 2001; 166:2472–2483. [PubMed: 11696814]
41. Mori CSK. Sexing of human embryos and fetuses by fluorescent in situ hybridization (FISH) to paraffin-embedded tissues with sex chromosome-specific DNA probes. *Am J Med Genet*. 1994; 150:180–186. [PubMed: 8010350]
42. Mani SAGW, Liao MJ, Eaton EN, Ayyanan A, Zhou AY, Brooks M, Reinhard F, Zhang CC, Shipitsin M, Campbell LL, Polyak K, Briskin C, Yang J, Weinberg RA. The epithelial-mesenchymal transition generates cells with properties of stem cells. *Cell*. 2008; 133:704–715. [PubMed: 18485877]
43. Moser FG, Dorman BP, Ruddle FH. Mouse-human heterokaryon analysis with a 33258 Hoechst-Giemsa technique. *The Journal of cell biology*. 1975; 66:676–680. [PubMed: 51024]
44. Moody SEPD, Pan TC, Sarkisian CJ, Portocarrero CP, Sterner CJ, Notorfrancesco KL, Cardiff RDCL. The transcriptional repressor Snail promotes mammary tumor recurrence. *Cancer Cell*. 2005; 8:197–209. [PubMed: 16169465]
45. Ansieau SBJ, Doreau A, Morel AP, Bouchet BP, Thomas C, Fauvet F, Puisieux I, Doglioni C, Piccinin S, Maestro R, Voeltzel T, Selmi A, Valsesia-Wittmann S, Caron de Fromental C, Puisieux A. Induction of EMT by twist proteins as a collateral effect of tumor-promoting inactivation of premature senescence. *Cancer Cell*. 2008; 14:79–89. [PubMed: 18598946]
46. Ben-Porath IYO, Benvenisty N. The *tmp* gene, encoding a membrane protein, is a c-Myc target with a tumorigenic activity. *Mol Cell Biol*. 1999; 19:3529–3539. [PubMed: 10207076]
47. Trimboli AJFK, de Bruin A, Wei G, Shen L, Tanner SM, Creasap N, Rosol TJ, Robinson ML, Eng C, Ostrowski MC, Leone G. Direct evidence for epithelial-mesenchymal transitions in breast cancer. *Cancer Res*. 2008; 68:937–945. [PubMed: 18245497]

48. Yang JWR. Epithelial-mesenchymal transition: at the crossroads of development and tumor metastasis. *Dev Cell*. 2008; 14:818–829. [PubMed: 18539112]
49. Al-Hajj M, Wicha MS, Benito-Hernandez A, Morrison SJ, Clarke MF. Prospective identification of tumorigenic breast cancer cells. *Proc Natl Acad Sci U S A*. 2003; 100:3983–3988. [PubMed: 12629218]
50. Patrawala L, Calhoun T, Schneider-Broussard R, et al. Highly purified CD44+ prostate cancer cells from xenograft human tumors are enriched in tumorigenic and metastatic progenitor cells. *Oncogene*. 2006; 25:1696–1708. [PubMed: 16449977]
51. Woodward WA, Sulman EP. Cancer stem cells: markers or biomarkers? *Cancer metastasis reviews*. 2008; 27:459–470. [PubMed: 18437295]
52. Morel APLM, Thomas C, Hinkal G, Ansieau S, Puisieux A. Generation of breast cancer stem cells through epithelial-mesenchymal transition. *PLoS ONE*. 2008; 3:e2888. [PubMed: 18682804]
53. Ahmed FSJ, Herbert JM, Steven NM, Bicknell R. Tumor stroma as a target in cancer. *Curr Cancer Drug Targets*. 2008; 1:447–453. [PubMed: 18781891]

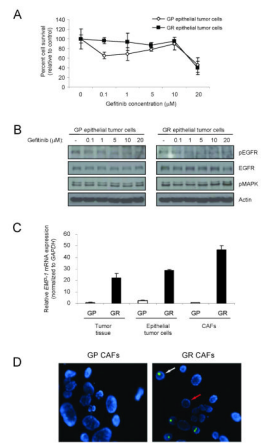


Figure 1.

A, GP and GR epithelial tumor cells are equally responsive to gefitinib. Equal numbers of GP and GR epithelial tumor cells seeded in 96-well plates were treated in quadruplicates with increasing concentrations of gefitinib (0, 0.1, 1, 5, 10 and 20 μ M) for 5 days. End point cell viability was measured using the MTS assay and the data are represented as a percentage of the untreated sample. B, Same as in A, except cells from 60mm dishes were lysed and analyzed by immunoblot for pEGFR, EGFR, pMAPK, and β -actin. C, hEMP-1 is expressed in the GR CAFs. Quantitative RT-PCR analysis of hEMP-1 mRNA comparing GP to GR in the tumor tissue, epithelial tumor cells, and CAFs. Data are normalized to GAPDH and presented as fold induction of GP tumor tissue. D, FISH analysis of purified GP and GR CAFs with CEP Y (DYZ1) probe (green fluorescent signal) depicting human nuclei (white arrow) and murine nuclei (red arrow). Nuclear counter staining with DAPI (blue).

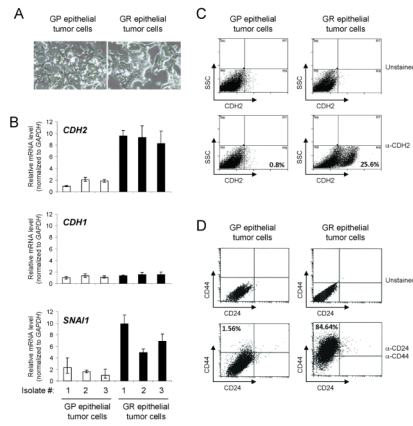


Figure 2. Increased expression of mesenchymal markers and CD44^{hi}/CD24^{lo} surface expression in GR epithelial tumor cells. *A*, Representative photomicrographs of GP and GR epithelial tumor cells. *B*, Relative mRNA expression of human *CDH2* (*top panel*), human *CDH1* (*middle panel*), and human *SNAI1* (*bottom panel*) in GP and GR epithelial tumor cells from three different tumor isolates. Data are normalized to *GAPDH* and presented as fold expression. *C*, Flow cytometry comparing CDH2 cell surface expression in GP and GR epithelial tumor cells. *D*, Flow cytometry comparing CD44 and CD24 cell surface expression in GP (*left*) and GR (*right*) epithelial tumor cells. The percentage of positive cells is indicated in the respective quadrants.

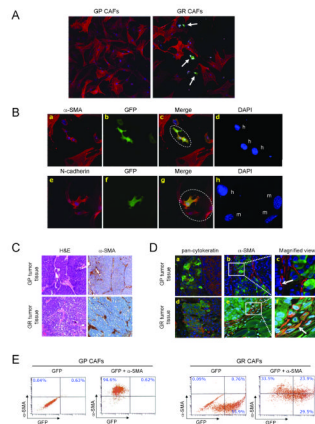


Figure 3.

In vivo demonstration of EMT in GFP tagged tumors. **A**, Immunocytochemistry for α -SMA in GP (left) and GR (right) purified CAFs. Multiple cells dual positive for GFP and α -SMA are indicated (white arrows, right panel). **B**, Immunocytochemistry for CAF sub-population dual positive for GFP and α -SMA (a–d) or N-cadherin (e–h). DAPI stained human (h) or murine (m) nuclei are shown in (d and h). (d and h) represent enlarged views for regions outlined in (c and g), respectively. Images were acquired at 20 \times (A) or 60 \times (B) and analyzed in Adobe Photoshop. **C**, Hematoxylin and eosin (H&E) and α -SMA immunohistochemistry on GP and GR tumor tissues. **D**, Immunohistochemistry for the GFP expressing GP and GR tumor tissue. GP and GR tumor tissues were co-immunostained with antibodies against GFP and pan-cytokeratin (a and d), or GFP and α -SMA (b and e). (c and f) represent the enlarged images for regions outlined in (b and e), respectively. Images were acquired at 10 \times magnification (a and d) or 60 \times magnification (b and e). White arrows indicate the positive α -SMA staining in GP tumor sample (c) and overlap of GFP and α -SMA staining in GR tumor sample (f). **E**, Flow cytometry for α -SMA and GFP to estimate the percentage of dual positive GR CAFs. Percentage of positive cells is indicated in the respective quadrants.

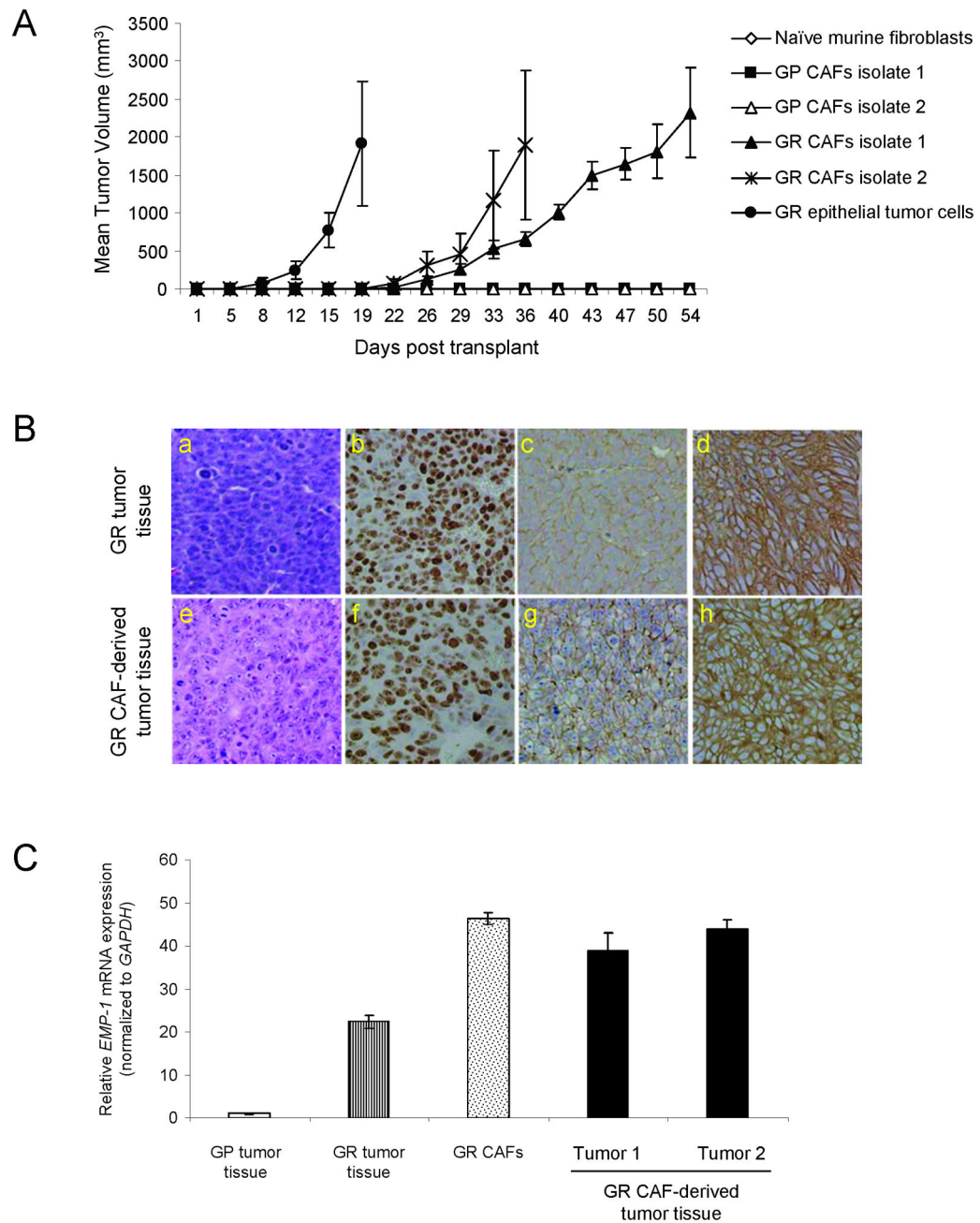
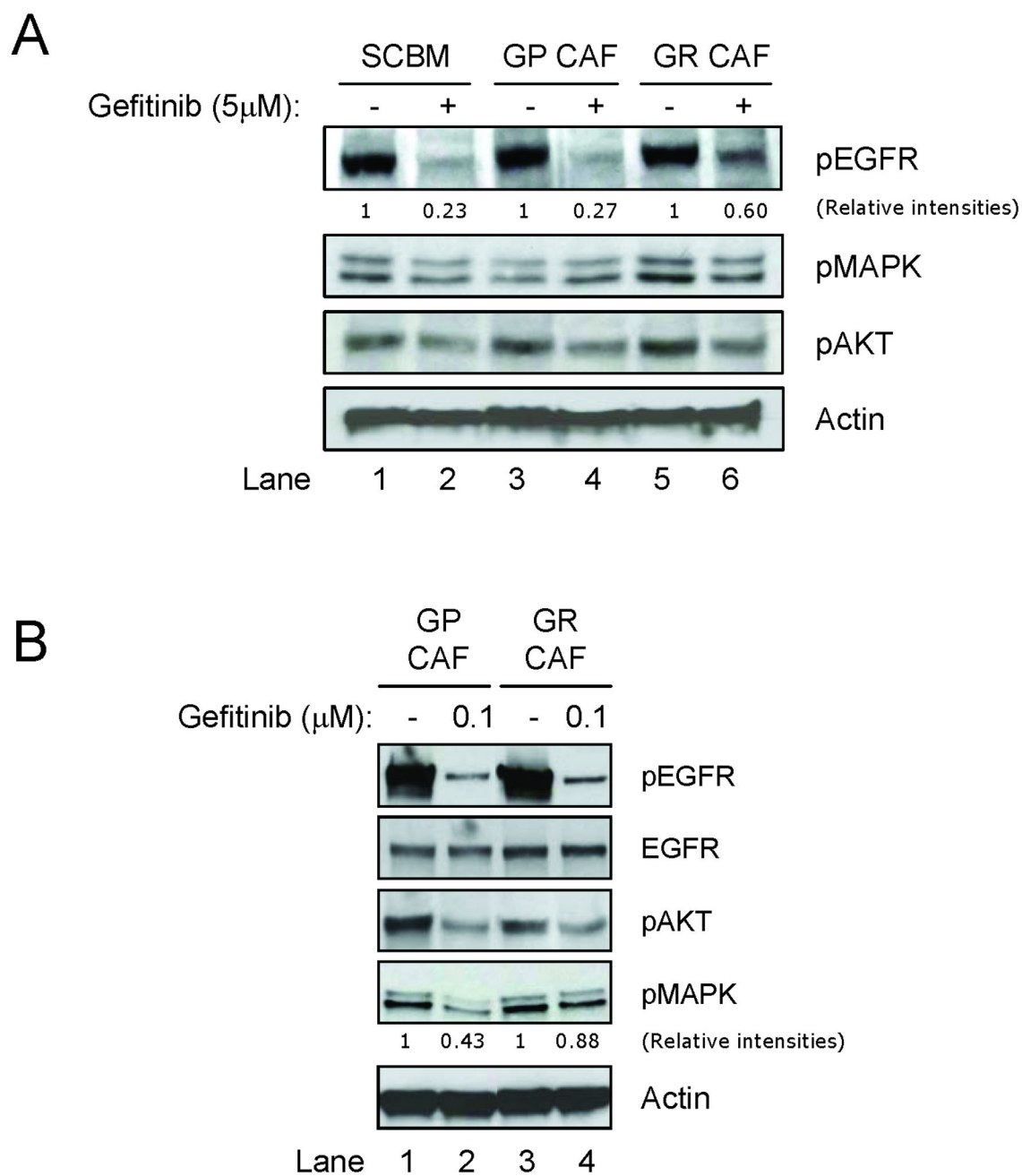


Figure 4.

Tumorigenicity of GR CAFs. **A**, Tumor growth curves of tumors derived from purified GP and GR CAFs. Purified GR epithelial tumor cells and naïve murine fibroblasts are used as positive and negative controls, respectively. Mean tumor volumes are plotted against time in days. Note the delay of ~14 days before the appearance of the GR CAF-derived tumors. **B**, GR tumor tissue (*top*) and GR CAF-derived (*bottom*) tumor tissue were stained with H&E (*a, e*) or antibodies against Ki67 (*b, f*), E-cadherin (*c, g*), or human-specific pan-cytokeratin (*d, h*). **C**, Quantitative RT-PCR analysis of *hEMP-1* mRNA from GP and GR tumor tissues, GR CAFs, and two different GR CAF-derived tumor tissue isolates. Data are presented as fold induction relative to GP tumor tissue.

**Figure 5.**

GR CAFs modulate the EGFR-TKI response in co-cultured tumor cells. *A & B*, Immunoblots for pEGFR, pMAPK and pAkt in GP epithelial tumor cells (*A*) and HCC827 cells (*B*) demonstrating effect of gefitinib treatment upon co-culture with GP or GR CAFs. Densitometric intensities for each marker were determined and the marker that demonstrates the most dramatic modification in each cell type in presence of gefitinib is presented.